Investigating Compton Scattering

Kye B. Choo

***Abstract*—In this experiment, the Compton effect was verified by measuring the dominant peak energy of a Cesium-137 source at various incident angles. The Klein-Nishina formula was then explored by investigating how the differential cross-section changes with incident angle. The results were compared to expected theoretical values and by simple simulation.**

I. Introduction

WHEN a photon (specifically a gamma ray in this experiment) interacts with an electron, there would be a transfer of momentum between the colliding photon and the electron. The scattered photon would not only change its direction of motion but also its wavelength and thus its energy. [1] The relationship between the scattering angle and the change in energy of the photon is summarised with the equation:

$$E_\gamma(\theta) = \frac{E_{\gamma 0}}{1 + \frac{E_{\gamma 0}}{mc^2}(1 - cos(\theta))} \tag{1}$$

When a photon scatters off an electron, there is also a forward bias in the scatter angle. This was observed by Compton himself [1] and later on formalised by Klein and Nishina [2]. The probability of scattering at a certain angle is known as the differential cross-section and its relationship is given by:

$$\frac{d\sigma}{d\Omega} = \frac{1}{2} r_e^2 \left(\frac{\lambda}{\lambda'}\right)^2 \left[\frac{\lambda}{\lambda'} + \frac{\lambda'}{\lambda} - sin^2(\theta)\right] \tag{2}$$

In the following sections, we aim to explore and verify the two above relationships.

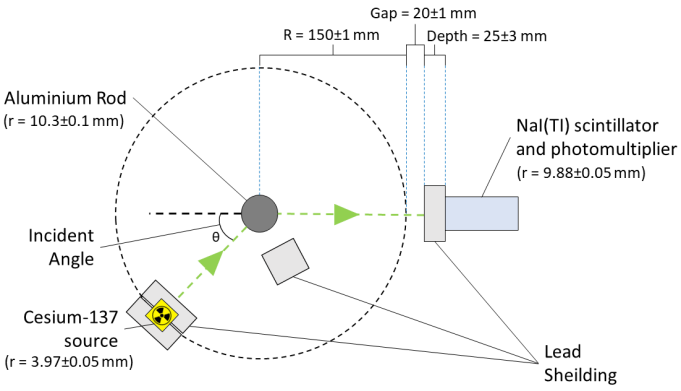

Fig. 1: A simple diagram illustrating the set up of our experiment. The source was moved around along the radius of the dashed circle to change the scattering angle.

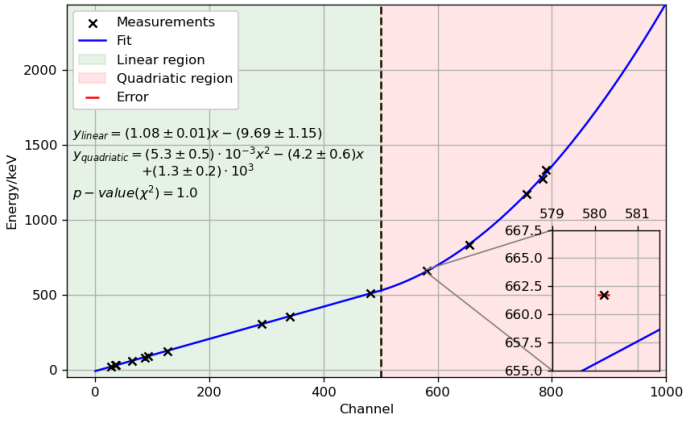

Fig. 2: Scaling used for this experiment. The green region is fitted with a straight line while the red region is fitted with a quadriatic curve. The fit returns a p-value of 1.0 when tested with a Chi-square goodness-of-fit test.

II. Methodology

Our experiment was set up as shown in Figure 1. The source used was a Cesium-137 source with a peak emmision of 661.7keV, and the NaI(TI) scintillator and photo-multiplier used was manufactured by Saint-Gobain with model 38-S-51.

In this experiment, the NaI(TI) scintillator and photomultiplier tube was used to take measurement, which is then sent to a multichannel analyser. With the CassyLab application, the signal is organised into un-scaled channels. Using multiple sources of radiation with known peak emission energies[1], the scaling was done using a piece-wise function consisting of a linear region and a quadriatic region. The choice of cut-off was done digitally with the aim of minimising the least-squares. This is shown in Figure 2.

The dataset for our experiment was obtained by moving the source by increments of 5 to 10 degrees between 10 degrees and 140 degrees. The background reading was taken right after each dataset, and the ”true” signal would be the measurement subtracted by the background. In order to reduce background noise, extra precaution was taken to place lead sheilding between the source and the detector.

III. Data and Analysis

After accounting for background noise, the dataset obtained is shown in Figure 3. It is noticeable that the relationship given by Compton’s equation holds quite well especially for higher scattering angles. To further verify Equation 1, the dataset was re-organised into the form [3]:

[1]Refer to Appendix B for list of sources used for scaling.

$$\frac{1}{E_\theta} - \frac{1}{E_0} = \frac{1}{m_e c^2}\left[1 - cos(\theta)\right] \tag{3}$$

In Figure 4, if Equation 3 holds, the gradient should be given by $\frac{e}{m_e c^2} \approx 1.96 \times 10^{-6}$. Since the fitted gradient from experimental data is $(1.9 \pm 0.1) \times 10^{-6}$, the data from this experiment supports Compton's equation.

By investigating how the radiation counts fall as different scattering angles were used, Klein-Nishina's equation was tested against our data. This is shown in Figure 5 where it could be seen that the general distribution of the differential cross-section follows the theoretical distribution. However, there is a vertical shift.

IV. Discussion

A. Comptom Effect

In general, the measured data agrees with the theoretical predictions quite well. The exception of low angles could be attributed to emmited photons from the source hitting the detector directly. This could be resolved by positioning two lead blocks with a pinhole before and after the scattering target. A good low-angle dataset was obtained through this method using the Americium-241 source. However, this was not done for the Cesium source because the count rate falls to negligible (smaller than noise) values if multiple pinholes were used, since the Cesium source available has a far lower activity than the Americium source available in the lab.

B. Differential Cross-Section

Our measured dataset (shown in blue in Figure 5) seems to have been shifted vertically downwards when compared to theoretical values, suggesting that the measured counts are lower than the theoretical counts. A possible explanation for this would be our failure to account for attenuation in air[2]. Although we have already accounted for the efficiency of the detector, it might be possible that our scaling factor is not accurate or that it might have different efficiencies for different energies.

A suggestion would be to redo the experiment by having the source and detector closer to the scattering target. By doing so, angular resolution is sacrificed for higher counts, which could help reduce the effects of noise and make it possible for further analysis.

We could also use smaller increments in angle. This makes the differential cross-section calculation more stable since it uses the derivative of our measurements. By using smaller increments, we could reduce the fluctuation.

V. Conclusion

In this experiment, the Compton Effect has been verified satisfactorily (as shown in Figure 3 and Figure 4) and the Klein-Nishina equation has been investigated adequately. Our findings was compared to a rough simulation and it is seen that our data falls within the limits of the simulated's range of output data.[3]

[2]Refer to Appendix C for mean-free-path estimates.
[3]Refer to Appendix D for comparison to simulation.

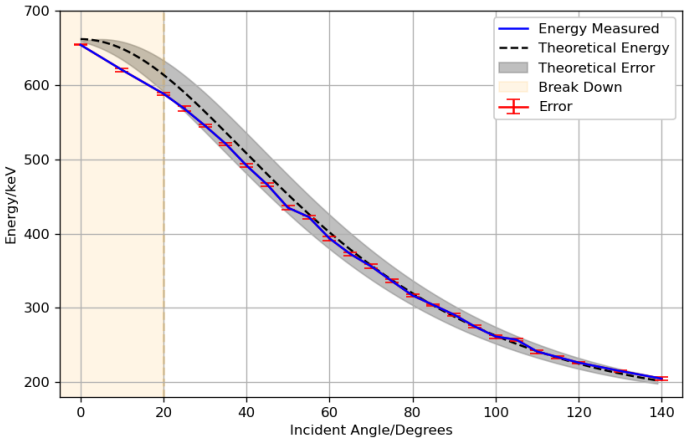

Fig. 3: The dataset of measured energies, along with theoretical energies and errors. The relationship given by Equation 1 breaks down at low angles.

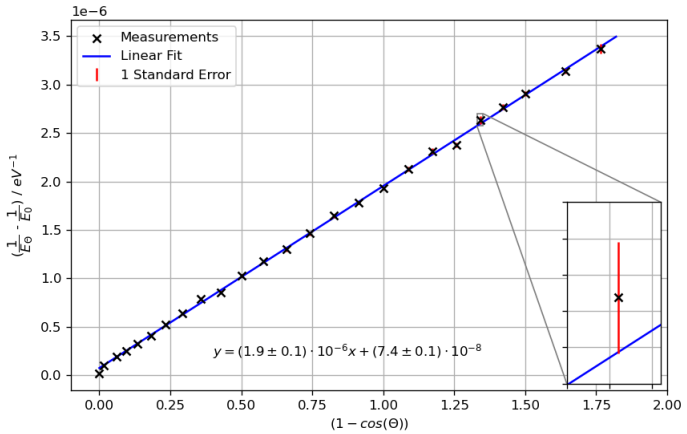

Fig. 4: Alternative plot of the dataset, showing a strong linear fit with p-value of 1.0 and gradient of $(1.9 \pm 0.1) \times 10^{-6}$.

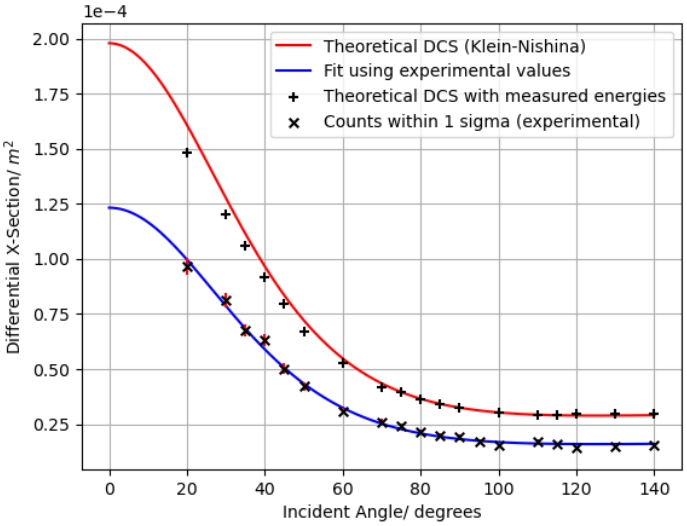

Fig. 5: A plot of the differential cross-section against scattering angle. The distribution follows the theoretical trends with a vertical shift.

APPENDIX A
FEEDBACK FROM LAST LAB CYCLE

Slides were well constructed with content presented in a clear and concise manner. You made good use of visual aids with correctly formatted tables and figures, the insets in particular were useful to highlight key features in the data. Good background equations and detail of the experiment was provided - although it would have been helpful to spend one or two sentences or a diagram explaining the basic photo-electric effect itself then detail the underlying theory. In-depth analysis sections demonstrated strong technical capabilities. Results comparing the different processing techniques used were insightful. Good automation of set-up. Inclusion of an experimental system diagram would have been helpful to support the preliminary and methodology sections. Conclusion slide was more a summary of results but did not express any take-away conclusions. Good to have the suggestions for improvement - maybe re-title slide to "Summary and Suggestions for Improvement" would better match slide content.

APPENDIX B
LIST OF SOURCES USED FOR SCALING

TABLE I: Sources used for calibration

Source	Channel	Energy/keV	Error/keV
Barium-133	35.30	30.85	0.04
Barium-133	86.4	81.0	0.1
Barium-133	291.5	303.0	0.6
Barium-133	341.4	356.0	0.3
Sodium-22	481.7	511.0	0.2
Sodium-22	783.5	1274.5	0.2
Cobalt-57	125.8	122.0	0.3
Cesium-137	36.6	32.0	0.3
Cesium-137	580.2	661.7	0.1
Cadmium-109	27.5	22.0	0.1
Cadmium-109	92.9	88.0	0.5
Americium-241	63.9	59.5	0.1
Cobalt-60	790.4	1332.0	0.3
Cobalt-60	755.9	1173.0	0.2

APPENDIX C
MEAN-FREE-PATH CALCULATIONS

A rough mean-free-path calculation was made to determine the suitability of our assumption that the ray does not interact in air, and that collisions happens only once in the scattering target.

The following mass attenuation coefficients, κ, was obtained from the National Institute of Standards and Technology's NIST-XCOM simulation. We assume our ray has an energy of 0.6 MeV, this is a valid approximation since this is only a rough calculation. For the XCOM simulation, we also assume that air composes of 78% Nitrogen molecules (N_2) and 21% Oxygen molecules (O_2).

$$\kappa_{air} = 8.042 \times 10^{-2} \left[\frac{cm^2}{g}\right] \tag{4}$$

$$\rho_{air} = 1.225 \times 10^{-3} \left[\frac{g}{cm^3}\right] \tag{5}$$

The linear attenuation coefficient, μ, is given by the product of the mass attenuation coefficient and the density. The mean-free-path estimate would be the reciprocal of the linear attenuation coefficient. [4]

$$\mu_{air} = 9.86 \times 10^{-5} \left[cm^{-1}\right] \tag{6}$$

$$MFP_{air} = \frac{1}{\mu_{air}} \approx 1 \times 10^4 \, [cm] \tag{7}$$

As seen from above, the mean-free-path of a gamma ray at 0.6 MeV is far greater than the length scales used in our experiments, which is about 30cm. Therefore, it is a safe assumption to say that the ray does not interact with air.

The same calculations could be done to estimate the interaction of the ray with our aluminium target:

$$\kappa_{Al} = 7.762 \times 10^{-2} \left[\frac{cm^2}{g}\right] \tag{8}$$

$$\rho_{Al} = 2.7 \left[\frac{g}{cm^3}\right] \tag{9}$$

$$\mu_{Al} = 0.4 \left[cm^{-1}\right] \tag{10}$$

$$MFP_{Al} \approx 2.5 \, [cm] \tag{11}$$

Since our target has a radius of 1.03cm, we can still make the assumption that there is only one collision per photon with the aluminium atoms, although this assumption would not be as strong as the previous one.

APPENDIX D
SIMULATIONS

To do a sense-check of our measured data, we did a rough simulation (a not-very-good-simulation) of the measured energies after collision. The method used is a monte-carlo simulation [5], where the source is assumed to be a circular disc with uniform probability of a 661.7 keV photon emission originating from any surface element on the disc.

To check that the source is simulated properly, a source of radius r and a square of sides 2r were defined. If the source is sensible, the proportion of emissions within the circle compared to the square would be the ratio of areas, $\frac{\pi r^2}{(2r)^2} \approx 0.785$. This was found to be true,

The photons were assumed to be collimated and were allowed to travel in a straight line towards the target, assuming that there is no interaction with air (refer to Appendix C). The simulated photons were allowed to collide only once with the target, and the collision was not limited to the surface of the target but also anywhere within the target. Since the mean-free-path of the 662 keV photon in aluminium is larger than the radius of the target, the assumption was made that there is a uniform probability of interaction anywhere within the target.

The scattered photon is then allowed to change energy and direction according to Compton's Equation (1), and it travels the remaining path towards the detector. The energy is recorded if the photon strikes within the circular disc defined as the detector.

In our simple simulation, it is found that the measured peak energies falls within the upper and lower limits of the simulated energies for higher angles. However for lower angles, the simulated data does not match the measured data that well. This could be seen in an extract of one of the plots for 90 degrees scattering.

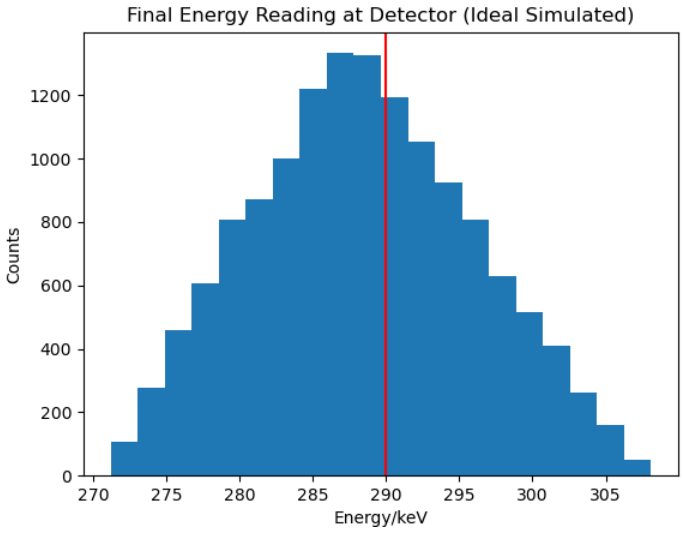

Fig. 6: The above data is for a 90 degrees scattering. The blue bins are the number of counts of measured photons at each energy bins. The red line would be the dominant energy peak at the same corresponding scattering angle. It is seen that the measured peak energy falls within the highest and lowest energies in the simulated data. However the form of the peak does not match that of the simulated data that well. This could be attributed to the many assumptions made in the simulation particularily the assumptions regarding uniform probabilities.

REFERENCES

[1] A. H. Compton, "A quantum theory of the scattering of x-rays by light elements," *Physical Review*, vol. 21, no. 5, p. 483–502, 1923.

[2] O. Klein and Y. Nishina, "On the Scattering of Radiation by Free Electrons According to Dirac's New Relativistic Quantum Dynamics," in *The Oskar Klein Memorial Lectures, Vol. 2*, 1994, pp. 113–129.

[3] J. E. Parks and C. P. Cheney. Compton scattering of cs-137 gamma rays. [Online]. Available: http://www.chm.bris.ac.uk/webprojects2003/swinerd/equation/

[4] B. D. e. a. Priamo F, Chieng R. Linear attenuation coefficient. [Online]. Available: https://radiopaedia.org/articles/linear-attenuation-coefficient?lang=gb

[5] A. Bazza, A. El Hamli, M. Hamal, A. Moussa, M. Zerfaoui, L. Hamam, M. Ouchrif, and Y. Taylati, "Nai(tl) detector response at different energies and a validation with monte carlo simulation," in *Advances in Smart Technologies Applications and Case Studies*, A. El Moussati, K. Kpalma, M. Ghaouth Belkasmi, M. Saber, and S. Guégan, Eds. Cham: Springer International Publishing, 2020, pp. 647–655.